Critical phenomena in chiral symmetry breakdown of micromagnetic configurations in a nanostructured ferromagnetic ring

E. Saitoh,[1] K. Harii,[1] H. Miyajima,[1] T. Yamaoka,[2] and S. Okuma[3]
[1]*Department of Physics, Keio University, Hiyoshi, Yokohama 223-8522, Japan*
[2]*SII Nano Technology Inc., Takatsuka, Matsudo, 270-2222, Japan*
[3]*Research Center for Low Temperature Physics, Tokyo Institute of Technology, Meguro, Tokyo, 152-8551, Japan*
(Received 21 October 2004; revised manuscript received 22 February 2005; published 25 May 2005)

Nanostructured ferromagnets provide a variety of well-defined magnetization configurations. The symmetry of these configurations in a ferromagnetic nanostructured ring can be altered by an external magnetic field in a controllable manner. We found, by means of resistive-noise spectroscopy, that the chiral-symmetry breakdown of a micromagnetic configuration accompanies a critical fluctuation of the magnetization distribution analogous to a second-order phase transition.

DOI: 10.1103/PhysRevB.71.172406 PACS number(s): 75.75.+a, 64.60.−i, 74.20.De, 75.60.Ch

Nanostructured ferromagnets are promising elements of spin electronics, since they provide a variety of well-defined magnetization configurations.[1] In a soft-ferromagnetic wire of nanoscale width, for example, the magnetization aligns parallel to the wire axis to reduce the demagnetization energy. In a ring made of the wire, the magnetization aligns along the circumference to form a flux-closure structure.[2–4] Since the flux-closure structure generates a minimal stray field and has an internal degree of freedom with respect to the magnetic chirality, that is, the clockwise or counterclockwise circulation of magnetization,[5] the rings show promise for use in high-density data storage systems including magnetic random-access memory.[6] Direct observations of these micromagnetic configurations have become possible with the development of techniques such as magnetic force microscopy (MFM). However, the formation dynamics of the micromagnetic configurations is still unclear experimentally, a problem which has limited the application of nanostructured magnets.

Among various magnetization configurations, the flux-closure state in nanostructured rings has the simplest structure with a nontrivial topology of magnetization distribution. The symmetry of the magnetization distribution in the rings can be changed continuously by an external magnetic field; applying a strong magnetic field perpendicular to the rings aligns the magnetization parallel to the field, while decreasing the field forms a flux-closure structure.[7] Elucidating the mechanism of this simplest transition between the uniform and the flux-closure structures is essential for understanding the general formation process of micromagnetic configurations as well as controlling them precisely in nanostructured ferromagnets. In this paper, to clarify the mechanism involved, the dynamics of the formation of a flux-closure structure in a soft-ferromagnetic $Ni_{81}Fe_{19}$ ring has been studied by means of resistivity-noise spectroscopy.

Resistivity in nanostructured ferromagnets reflects the magnetization configuration via magnetoresistance, and the dominant contribution to the magnetoresistance in $Ni_{81}Fe_{19}$ at room temperature is anisotropic magnetoresistance (AMR) effect.[8] However, precise measurement of the resistance noise for the whole ferromagnetic ring is difficult due to its high resistance. To measure the resistive noise in the ferromagnetic ring sensitively, a bridge circuit was built on the ring. Figure 1(a) shows a scanning electron micrograph of the ring system investigated in the present study. The system comprises a $Ni_{81}Fe_{19}$ ring of 100 nm width, Cu current electrodes, and voltage probes prepared by the following lift-off technique. First, a ZEP520 resist 100 nm in thickness is spin-coated on a thermally oxidized Si substrate. After the ring pattern is exposed by an electron-beam writer, the resist is developed. $Ni_{81}Fe_{19}$ is deposited in a vacuum by an electron-beam method, and then the resist is removed, producing a

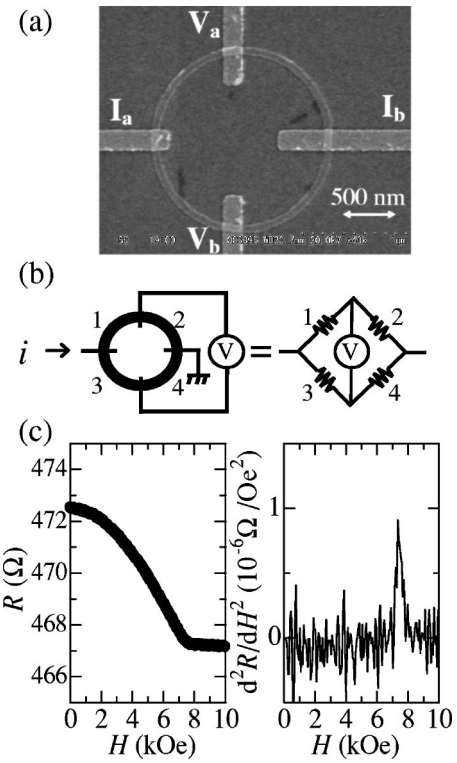

FIG. 1. (a) A scanning electron micrograph of the sample. The sample consists of a $Ni_{81}Fe_{19}$ ring, two Cu current electrodes ($\mathbf{I_a}$ and $\mathbf{I_b}$) and two Cu voltage probes ($\mathbf{V_a}$ and $\mathbf{V_b}$). The thickness of the $Ni_{81}Fe_{19}$ ring is 20 nm. (b) Schematic illustration of the measurement configuration equivalent to a built-in "Wheatstone-bridge" on the $Ni_{81}Fe_{19}$ ring. (c) Field H dependence of the resistance $R(H)$ and $d^2R(H)/dH^2$ measured using the current electrodes.

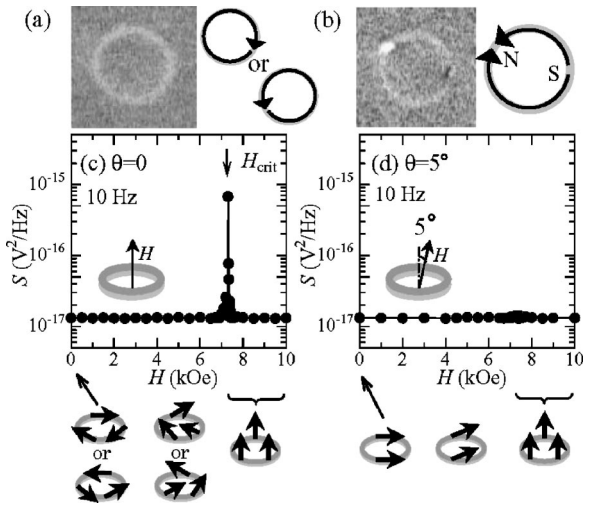

FIG. 2. (a),(b) Magnetic-force-microscope images for remanent magnetic states of the ring, and schematic illustrations of micromagnetic configurations deduced from the images. The directions of the initial magnetic field (7.5 kOe) are (a) perpendicular to the ring plane and (b) at the angle of 5° to the perpendicular of the ring. The black and white signals correspond to the stray field due to the S and N magnetic charge on domain walls. (c),(d) External-magnetic-field H dependence of the fluctuation spectral density of voltage V at 10 Hz between voltage probes $\mathbf{V_a}$ and $\mathbf{V_b}$, and schematic illustration of the magnetization process of the ring. The magnetic field is (c) perpendicular to the ring plane and (d) at the angle of 5° to the perpendicular direction of the ring. Before the measurement, a magnetic field of 7.5 kOe is applied and then the voltage noise is measured as the field is decreased. H_{crit} represents the external field strength at which the noise spectral density reaches a maximum.

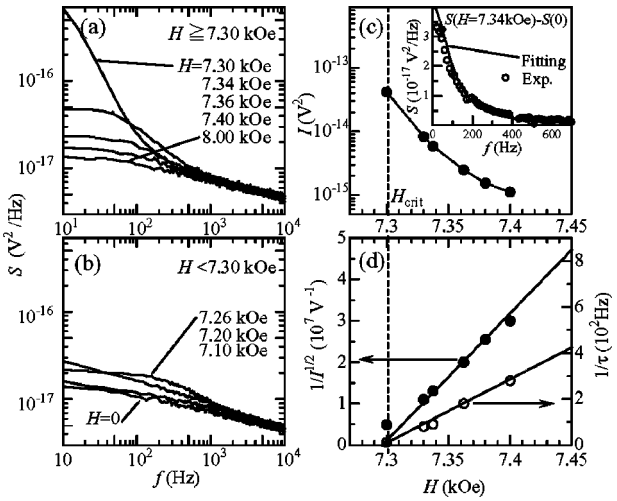

FIG. 3. (a),(b) Voltage V noise power spectra for a $Ni_{81}Fe_{19}$ ring at various external magnetic fields (a) $H \geqslant 7.3$ kOe and (b) $H < 7.3$ kOe measured by applying an electrical current of 100 μA. The magnetic field is perpendicular to the ring. (c) External-magnetic-field dependence of the integrated intensity I of the low-frequency noise-enhancement spectra $S(H)-S(H=0)$ above H_{crit} estimated by the Lorentzian-fitting procedure. The solid line is a visual guide. The inset shows the fitting curve (a solid line) for the measured spectrum (open circles) at 7.34 kOe. (d) External-magnetic-field dependence of $1/I^{1/2}$ (closed circles) and the spectral width $1/\tau$ (open circles) of the low-frequency noise-enhancement spectra $S(H)-S(H=0)$ above H_{crit} estimated by the Lorentzian-fitting procedure.

$Ni_{81}Fe_{19}$ ring 20 nm in thickness. The Cu electrodes are fabricated on the ring in the same way. MFM measurements showed that the remanent states after an application of a 7.5 kOe magnetic field perpendicular to the ring are flux-closure structures [see Fig. 2(a)]. We confirmed that the remanent states are randomly clockwise or counterclockwise using magnetoresistance measurements.[9] An electrical current of $i=100$ μA was applied through the current electrodes [$\mathbf{I_a}$ and $\mathbf{I_b}$, in Fig. 1(a)], and the noise in the voltage V across the two voltage probes [$\mathbf{V_a}$ and $\mathbf{V_b}$, in Fig. 1(a)] was monitored at 300 K using a differential preamplifier and a spectrum analyzer. Note that this circuit is equivalent to a "Wheatstone-bridge" circuit where the quarter-circles of the $Ni_{81}Fe_{19}$ ring correspond to the four resistors in the bridge, as shown in Fig. 1(b). Therefore, the flux-closure remanent states lead to $V \approx 0$, whereas a discrepancy of resistance among the quarter-circles gives rise to V as in the following equation:

$$V \approx \frac{i}{4}(\delta_1 + \delta_4 - \delta_2 - \delta_3). \quad (1)$$

Here, δ_n represents the difference between the resistance of the quarter-circle n shown in Fig. 1(b) and the averaged resistance of the quarter circles. By measuring V, this method allows sensitive detection of nonuniform local-resistance fluctuation in the ring.

Figure 1(c) shows the field dependence of the two-terminal resistance $R(H)$ of the sample measured using $\mathbf{I_a}$ and $\mathbf{I_b}$. From this data, we determined the magnetization-saturation field of the ring as 7.3 kOe, a field at which $d^2R(H)/dH^2$ peaks. Note that $d^2R(H)/dH^2$ should diverge to infinity at the magnetization saturation in an ideal uniform magnet with the axis of easy magnetization perpendicular to the field direction.[10]

Figure 2(c) shows the spectral density S of the noise power of the voltage V at 10 Hz as a function of the external magnetic field H applied perpendicular to the ring plane. After a magnetic field 7.5 kOe, a value greater than the magnetization saturation field of 7.3 kOe, is applied, the voltage noise is measured as the field is lowered. Notably, the noise power is remarkably enhanced around $H_{crit}=7.30$ kOe. This noise enhancement coincides with the magnetization saturation, a finding indicating that the enhancement is of magnetic origin. The noise disappears in the absence of the electrical current; evidently, the noise reflects resistive fluctuation. The frequency spectra of S for various values of H are shown in Figs. 3(a) and 3(b). Above H_{crit}, the noise enhancement, $S(H)-S(H=0)$, is well reproduced by the Lorentz functions; the fitting result is exemplified in the inset of Fig. 3(c). The integrated intensity I and the spectral width $1/\tau$ of $S(H)-S(H=0)$ above H_{crit} estimated from the fitting are shown in Figs. 3(c) and 3(d) as a function of H. Interestingly, both $1/I^{1/2}$ and $1/\tau$ decrease almost linearly as H drops towards H_{crit}. This implies that some magnetic instability lies at H_{crit}.

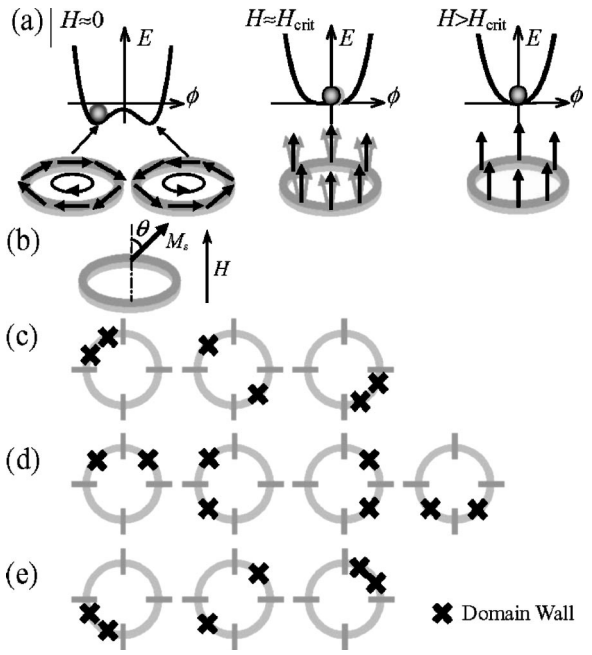

FIG. 4. (a) Schematic illustration of the magnetic-chiral-symmetry breakdown. The curves describe the magnetic energy as a function of the magnetic chirality of the ring. (b) Schematic illustration of the definition of θ, the angle between local magnetization and the direction perpendicular to the ring. (c),(d),(e) Possible configurations of a pair of nucleated domain walls in the ring. The crosses denote the domain-wall positions. The configurations (c), (d), and (e) give rise to positive, nearly zero, and negative values of V, respectively, via the bridge circuit.

The observed behaviors of $I^{1/2}$ and $1/\tau$ above H_{crit} are accounted for by the instability of magnetic-chiral-symmetry breakdown at H_{crit}. Hereafter, for simplicity, we treat the magnetic fluctuation on the mean-field level. The magnetic energy in the narrow ring under a magnetic field H perpendicular to the ring is simply approximated by a sum of the Zeeman energy and the demagnetization energy as in the following equation:

$$E(\theta) = -\mu_0 M_S H \cos\theta - \frac{\mu_0 N M_S^2}{2}\sin^2\theta, \tag{2}$$

where θ is the angle between the local magnetization and the direction perpendicular to the ring plane [see Fig. 4(b)]. M_S and N denote the saturation magnetization and the effective demagnetization factor, respectively. In the vicinity of the magnetization saturation, Eq. (2) can be expanded in a series of the magnetic-chiral degree of freedom $\phi \equiv \sin\theta$, that is, the solid angle subtended by the magnetic moments, as

$$\begin{aligned} E(\phi) &= -\mu_0 M_S H\sqrt{1-\phi^2} - \frac{\mu_0 N M_S^2}{2}\phi^2 \\ &= E(\phi=0) + \frac{\mu_0 M_S}{2}(H - NM_S)\phi^2 + \left(\frac{\mu_0 M_S H}{8}\right)\phi^4 \\ &\quad + \cdots . \end{aligned} \tag{3}$$

This equation is identical to Landau's phenomenological model of a second-order phase transition;[11,12] the magnetic-chiral symmetry above the magnetization saturation breaks down into a clockwise ($\phi>0$) or counterclockwise ($\phi<0$) circulation of magnetization at $H=NM_S$: the magnetization saturation field [Fig. 4(a)]. At this field, the curvature of $E(\phi)$ at $\phi=0, \partial^2 E(\phi=0)/\partial\phi^2$, becomes zero, which critically enhances fluctuation of ϕ. According to the fluctuation-dissipation theorem, the power of this fluctuation, $\langle\phi^2\rangle \propto \int_0^\infty I_\phi(f)\mathrm{d}f$, is proportional to the susceptibility of $\phi, \chi = \lim_{H_\parallel\to 0}(\phi/H_\parallel)$. Here, $H_\parallel$ denotes the conjugate field to ϕ, that is, the in-plane eddy magnetic field along the ring circumference, whose average is zero in our experimental setup. $I_\phi(f)$ and $\langle\cdots\rangle$ represent the power spectrum of ϕ and the time averaging, respectively. χ is calculated to be $\chi \propto (H-NM_S)^{-1}$ by minimizing[11] $E(\phi) - \mu_0 M_S H_\parallel \phi$. Since the resistivity change due to AMR[8] is proportional to $\sin^2\phi \approx \phi^2$, the fluctuation of ϕ generates a resistivity noise whose power is proportional to $(H-NM_S)^{-2}$. This situation accounts for the observed critical enhancement[13] of $I^{1/2}$ toward H_{crit}. According to the van-Hove's theory of the critical fluctuation,[11] time scale of the fluctuation of ϕ is proportional to χ, which is consistent with the observed critical suppression of $1/\tau$ proportional to $H-H_{\mathrm{crit}}$. Since fluctuations whose coherence is much shorter than the ring size hardly contribute to V, the observed noise can be specifically ascribed to magnetic-chiral fluctuation with a coherence length comparable to the ring size. This fluctuation causes a nonuniform but long-range AMR fluctuation which can be sensitively detected due to the built-in bridge circuit in the present system.[14] Such a long-range coherence of the fluctuation can initiate the formation of a domainless flux-closure structure. The above discussion neglects the effects of beyond-mean-field fluctuation and exchange energy, and its good agreement with the experimental results indicates a minor role of these effects in the present system.

The above analysis shows that the observed magnetic fluctuation is relevant to the symmetry transition of the micromagnetic configurations in the present ring, providing a direct analogy between the symmetry transition of micromagnetic configurations and a second-order phase transition. This suggestion is supported by the fact that the noise enhancement disappears by a tilting of the field direction slightly away from the perpendicular of the ring plane [see Fig. 2(d)], where the remanent state takes the multidomain structure shown in Fig. 2(b). Note that the symmetry of the multidomain magnetization configuration is identical to that of the uniformly magnetized state parallel to the tilted external-field above H_{crit}. This situation is in contrast to the case of the field perpendicular to the ring, where the chiral symmetry of magnetization distribution breaks down at H_{crit} to form a flux-closure magnetic structure. This is direct evidence of the close relationship between the observed fluctuation and the symmetry transition of magnetization distributions.

As H decreases below H_{crit}, as shown in Fig. 3(b), the noise intensity rapidly decreases and the spectra deviate from Lorentzians. The noise immediately below H_{crit} is characterized by a non-Gaussian telegraph-type wave form, as depicted in Fig. 5. With a further decrease in H, the telegraph-

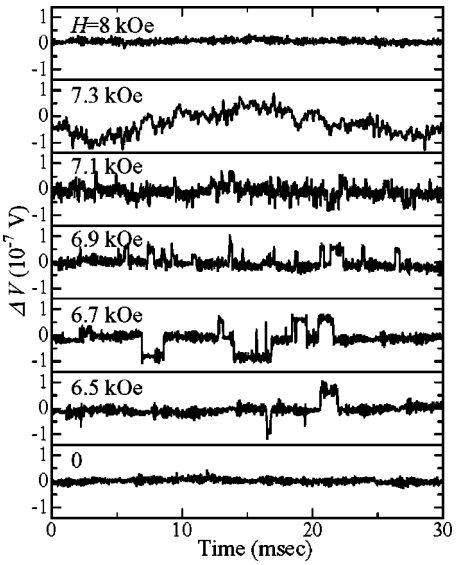

FIG. 5. Time evolution of the fluctuation in V (ΔV) from which the time-averaged V is subtracted. The external magnetic fields are perpendicular to the ring plane. The measurement is performed by applying an electrical current of 100 μA through the current electrodes.

type noise becomes scattered and then disappears below 6.5 kOe. This noise also disappears when the magnetic field is slightly tilted (e.g., 5°). The telegraph noise consists of the switching of V among three values, as typically observed at 6.7 kOe. This finding suggests that the telegraph noise is due to the thermal nucleation and annihilation of domains, because all the possible configurations of a pair of nucleated domain walls can be classified into three groups, illustrated in Figs. 4(c)–4(e); each of these groups gives rise to a different value of V via the bridge circuit described by Eq. (1). The thermal excitation of higher-energy states comprising more domain walls should be rare compared with these two-domain-wall states. The creation and annihilation of the three types of domain may be responsible for the observed switching of V among the three values.[15,16] The increase in the in-plane component of local magnetization of the ring as H decreases suppresses the domain-wall length and may change the property of the magnetic fluctuation from the long-range mode above H_{crit} to the domain-wall (soliton) mode below H_{crit}. In the field perpendicular to the ring plane, because of the degeneracy of the clockwise and counterclockwise configurations, the domain-wall nucleation loses only the domain-wall energy, which can be small,[15] immediately below H_{crit}, due to the small angle between the perpendicular direction to the ring plane and the local magnetization. The small domain-wall energy enhances the thermal nucleation and annihilation of domains. With a further decrease in H, the domain-wall energy increases and suppresses the domain nucleation.

In summary, we have investigated the resistivity noise in a ferromagnetic nanostructured ring in response to varying the external magnetic field. Around the magnetization saturation field H_{crit} perpendicular to the ring, we observed a critical enhancement of the noise, indicating a critical fluctuation of micromagnetic configurations relevant to the magnetic-chiral symmetry breakdown in the ring. This result demonstrates the close relationship between the continuous symmetry transition of micromagnetic configurations and magnetic fluctuation.

This work was supported by a Grant-in-Aid from the Ministry of Education, Science, Sports, and Culture, of Japan and the Foundation Advanced Technology Institute. The authors thank G. Tatara for discussion.

[1] For a review, see, for example, R. Skomski, in *Spin Electronics*, edited by M. Ziese and M. J. Thornton (Springer, Berlin, 2001).
[2] S. P. Li, D. Peyrade, M. Natali, A. Lebib, Y. Chen, U. Ebels, L. D. Buda, and K. Ounadjela, Phys. Rev. Lett. **86**, 1102 (2001).
[3] M. Kläui, J. Rothman, L. Lopez-Diaz, C. A. F. Vaz, J. A. C. Bland, and Z. Cui, Appl. Phys. Lett. **78**, 3268 (2001).
[4] F. J. Castano *et al.*, Phys. Rev. B **67**, 184425 (2003).
[5] R. Skomski, J. P. Liu, and D. J. Sellmyer, Phys. Rev. B **60**, 7359 (1999).
[6] J-G. Zhu, Y. Zheng, and G. A. Prinz, J. Appl. Phys. **87**, 6668 (2000).
[7] S. Kasai, T. Niiyama, E. Saitoh, and H. Miyajima, J. Magn. Magn. Mater. **239**, 228 (2002).
[8] T. R. McGuire and R. I. Potter, IEEE Trans. Magn. **MAC-11**, 1018 (1975).
[9] K. Harii, E. Saitoh, H. Miyajima, and T. Yamaoka, J. Magn. Magn. Mater. **282**, 19 (2004).
[10] See, for example, S. Chikazumi, *Physics of Ferromagnetism*, 2nd ed. (Oxford University Press, Oxford, 1997).
[11] See, for example, P. C. Hohenberg and B. I. Halperin, Rev. Mod. Phys. **49**, 435 (1977).
[12] M. A. Pinto, Phys. Rev. Lett. **59**, 2798 (1987).
[13] Conventional van-Hove relaxation (Ref. 11) of ϕ based on Eq. (3) is consistent with the observed Lorentzian noise.
[14] For a rough estimate of the noise amplitude due to the AMR effect and long-range magnetic fluctuation, we calculated the integrated noise power (I) of V from the measured value of the magnetization and the AMR ratio (1%) using Eq. (3) and the fluctuation-dissipation theorem, assuming the fluctuation of ϕ in a quarter-circle of the ring immediately above the magnetization saturation. The calculated value of $I^{-1/2}(H-NM_S)^{-1}$ is 3.8×10^5 V^{-1} Oe^{-1}, which is comparable to the experimentally obtained value (3.1×10^5 V^{-1} Oe^{-1}): the slope of the $1/I^{1/2}$ vs H curve shown in Fig. 3(d).
[15] We estimated the energy of a pair of domain walls (DWs) at 6.9 kOe and 6.5 kOe using a micromagnetic simulator (OOMMF, http://math.nist.gov/oommf/). The result shows that the DWs are in-plane transverse type (see, for example, Ref. 16). The estimated energy values are $\approx$800 K and $\approx$1100 K, respectively. At these fields, the DW widths were estimated at $\approx$600 nm and $\approx$350 nm, respectively, shorter than a quarter of the circumference of the ring. $|\Delta V|$ due to a pair of nucleated domain walls was estimated at $\approx5\times10^{-8}$ V for both the field values. For this calculation, the AMR ratio is assumed to be 1% [see Fig. 1(c)]. All these results are consistent with the domain nucleation and annihilation scenario.
[16] E. Saitoh, H. Miyajima, T. Yamaoka, and G. Tatara, Nature (London) **432**, 203 (2004).